Available online at www.sciencedirect.com
ScienceDirect
Polymer 49 (2008) 610–620
polymer
www.elsevier.com/locate/polymer

Effects of acid- and diamine-modified MWNTs on the mechanical properties and crystallization behavior of polyamide 6

H. Meng [a], G.X. Sui [a,*], P.F. Fang [b,*], R. Yang [a]

[a] *Institute of Metal Research, Chinese Academy of Sciences, 72 Wenhua Road, Shenyang 110016, China*
[b] *Physics Department, Wuhan University, Wuhan 430072, China*

Received 13 July 2007; received in revised form 30 November 2007; accepted 1 December 2007
Available online 5 December 2007

Abstract

The acid- and diamine-modified multi-walled carbon nanotubes were characterized by XPS, apparent density test and SEM. Their effects on the mechanical properties and crystallization behavior of polyamide 6 (PA6) were comparatively investigated via SEM, DMA, tensile test and DSC. It was revealed that acid treatment could effectively induce polar oxygen-containing groups on the surface of MWNTs, which was beneficial for MWNTs to combine with polar PA6 matrix. However, the interactions such as the hydrogen bonds among the acid-modified MWNTs caused a compact stacking morphology, resulting in a worse dispersion in PA6 matrix. Further diamine modification on the acid-modified MWNTs could graft diamine molecules onto the surface of MWNTs, which weakened the interactions among the MWNTs and thus resulted in a less compact stacking morphology compared with acid-modified MWNTs. Therefore, a better dispersion and a stronger interfacial adhesion of MWNTs in PA6 matrix could be obtained with diamine-modified MWNTs. The storage modulus, glass transition temperature, yield strength, Young's modulus and crystallization temperature of PA6 were found to be improved significantly by the incorporation of diamine-modified MWNTs.

Keywords: Carbon nanotubes; Chemical modification; Polyamide 6

1. Introduction

Since the discovery of carbon nanotubes (CNTs) in 1991 by Iijima [1] and the practical realization of their extraordinary mechanical properties, extensive research related to the use of CNTs as nano-fillers to produce polymer nanocomposites has been increasingly conducted [2–7]. It is reported that CNTs possess theoretical Young's modulus and tensile strength as high as 1 TPa and 200 GPa, respectively, with an aspect ratio of 1000 [8,9]. All of these coupled with their nanoscale size and small density have made them the ideal reinforcement for polymers. However, over the past 16 years, the potential of CNTs as reinforcement for polymers has not been fully realized: the mechanical properties of derived composites have fallen short of predicted values [6]. An acceptable understanding of the discrepancy between the theory and experiment is that a sufficient dispersion of CNTs within polymer matrices and perfect interfacial adhesion between CNTs and polymer matrices in the processing of these nanocomposites has not been achieved.

It is well known that CNTs have exceptionally high aspect ratio, high surface area and intrinsic van der Waals attraction among tubes resulting in their significant agglomeration, thus it is difficult to achieve homogeneous dispersion in polymer matrices. On the other hand, the nonreactive surface of CNTs leads to a weaker interfacial adhesion with polymer matrices, which hinders efficient load transfer from polymer matrices to CNTs [10]. Therefore, the key issues for CNTs to reinforce polymer matrices are (a) homogeneous dispersion in polymer matrices without agglomeration and entanglement and (b) strong interfacial adhesion with polymer matrices, especially chemical interactions [10,11].

* Corresponding authors.
E-mail addresses: gxsui@imr.ac.cn (G.X. Sui), fangpf@whu.edu.cn (P.F. Fang).

0032-3861/$ - see front matter © 2007 Elsevier Ltd. All rights reserved.
doi:10.1016/j.polymer.2007.12.001

In order to overcome these issues, chemical modification of the surface of CNTs has been widely adopted, such as the acid treatment of CNTs as well as further modification of acid-modified CNTs with amines [12–22]. Han et al. [12] modified MWNTs using concentrated nitric acid, pristine and carboxylated multi-walled carbon nanotubes (MWNT and MWNTCOOH) were then incorporated into PA6 via in situ polymerization. They reported that MWNT and MWNTCOOH were well dispersed in PA6 matrix. By adding only 0.5 wt% MWNTs, the tensile strength of PA6/MWNT and PA6/MWNTCOOH nanocomposites was enhanced by about 7.6% and 8.2%, respectively, and the storage modulus was also increased, particularly for PA6/MWNTCOOH. Moreover, the crystallization temperature and the degree of crystallinity of PA6 were increased. Liu et al. [15] fabricated acid-modified MWNT/PA6 nanocomposites by a simple melt compounding. A homogeneous dispersion of MWNTs and strong interfacial adhesion between PA6 and MWNTs were reported. At 1 wt% loading of acid-modified MWNTs, the yield strength and Young's modulus of PA6 were increased significantly by about 123.9% and 115.3%, respectively. Schulte et al. [19] treated MWNTs with oxidizing inorganic acids and further modified the oxidized MWNTs using multi-functional amine, and then the amine-modified nanotubes were embedded in the epoxy resin. Their study found that the chemical modification led to a reduced agglomeration of MWNTs and improved effectively the interaction between the nanotubes and the epoxy resin.

However, although numerous investigations were carried out on chemical modification of the surface of CNTs, very few studies have been published to comparatively discuss the influences of differently modified MWNTs on the same polymer matrix. Recently, Ma et al. [22] focused on the different influences of acid- and amine-modified MWNTs on the mechanical properties of polyimide via in situ polymerization. Their study showed that modified MWNTs had better dispersion in polyimide matrix and stronger interfacial interaction with polyimide matrix than unmodified MWNTs. With loading of MWNTs at 0.99 wt%, the tensile strength of polyimide was improved by about 7.8%, 6.9% and 21.6% using unmodified, acid- and amine-modified MWNTs, respectively. The Young's modulus was elevated by about 8.7%, 39.1% and 47.8%, respectively. Song et al. [23] investigated the effects of MWNTs with −OH or −COOH on the crystallization behavior of poly(ethylene oxide) by DSC. Their results showed that incorporation of MWNTs resulted in the decrease in the crystallization temperature and reduced the degree of crystallinity, especially MWNTs with −OH. With increasing concentration of MWNTs, the effect became stronger. These results were different from that in other semi-crystalline polymer systems. They thought that modified MWNTs had a significant influence on the C−O and C−H stretching vibrations of PEO, which could lead to the decrease in the crystallization temperature and the degree of crystallinity of PEO in the blends.

As mentioned above, it can be seen that chemical modifications of the surface of CNTs often lead to a better dispersion of CNTs in the polymer matrices and improved interfacial adhesion between the modified CNTs and the polymer matrices, which causes enhanced mechanical properties of polymer/CNT nanocomposites. However, for a given polymer, how to identify the most appropriate modification approach is a key issue that affects greatly the reinforcing efficiency of CNTs. Accordingly, studying the effects of differently modified CNTs on the same polymer matrix is significant.

Currently, three processing techniques are commonly used to fabricate polymer/CNT nanocomposites: solution compounding, in situ polymerization and melt compounding [12–39]. From the literature, it is easily found that the solution compounding and in situ polymerization are dominant; unfortunately, they are difficult and inconvenient to carry out for industrial applications. On the contrary, melt compounding would be the best simple and effective method from both economic and industrial perspectives, because this process makes it possible to fabricate high performance polymer nanocomposites at low cost and in commercial scale [40]. Therefore, from an industrial perspective it is very important to develop the processing technique of melt compounding for combination of CNTs with conventional thermoplastic polymers to improve the mechanical properties of polymer nanocomposites. To our knowledge, although many studies have focused on the fabrication techniques of polymer/CNT nanocomposites, few reports can be found in literatures regarding PA6/MWNT nanocomposites via a simple melt compounding.

In the present work, PA6/MWNT nanocomposites were prepared by simple melt compounding with a mini-extruder. In order to improve the dispersion of MWNTs in PA6 matrix and interfacial adhesion with PA6 matrix, MWNTs were modified using mixed high concentration acids. After the acid treatment, MWNTs were further modified with ethylenediamine (EDA). The surface state and microstructure transformation of MWNTs after modification were characterized by X-ray photoelectron spectroscopy (XPS), apparent density test and scanning electron microscopy (SEM). Dispersion of MWNTs in PA6 matrix and interfacial adhesion with PA6 matrix were evaluated by scanning electron microscopy (SEM) too. Moreover, the effects of unmodified (U-MWNTs), acid-modified (A-MWNTs) and diamine-modified MWNTs (D-MWNTs) on the dynamic mechanical properties, tensile properties and crystallization behavior of PA6 matrix were comparatively investigated by dynamic mechanical analysis (DMA), tensile test and differential scanning calorimetry (DSC). The reason why U-MWNTs, A-MWNTs and D-MWNTs had different influence on PA6 matrix was then discussed.

2. Experimental

2.1. Materials

Multi-walled carbon nanotubes (MWNTs) were purchased from Chengdu Organic Chemistry Co. Ltd., Chinese Academy of Sciences (purity >95%, diameter: 50–80 nm, length: 5–20 μm). Polyamide 6 (PA6) resin was a commercially available product of Baling Company, China Petroleum and Chemical Corporation. Its melt-flow index was 7.2 g/10 min

(230 °C, 2.16 kg). Concentrated sulfuric acid (H_2SO_4, 98%), concentrated nitric acid (HNO_3, 65%), thionyl chloride ($SOCl_2$), tetrahydrofuran (THF) and ethylenediamine (EDA) were obtained from Shanghai Reagents Co. and used as-received.

2.2. Acid modification of MWNTs

As-received MWNTs (U-MWNTs, 1 g) were dispersed in 400 ml mixture of concentrated sulfuric and nitric acids (3:1 by volume). After being ultrasonicated for 1 h at room temperature (RT), the suspension was stirred for 4 h at 70 °C. It was then washed using deionized water and vacuum-filtered through 0.22 μm millipore PTFE membranes until the pH of the filtrate was ca. 7. The filtered solid was dried in a freeze drier, yielding acid-modified MWNTs (A-MWNTs).

2.3. Diamine functionalization of MWNTs

A-MWNTs (1 g) was suspended in 100 ml $SOCl_2$ with an ultrasonicator for 1 h at RT and then stirred for 24 h at 65 °C. The suspension was vacuum-filtered through PTFE membranes, washed with anhydrous THF, and dried under vacuum at RT for 1 h. The obtained MWNTs–COCl powders were immediately added into excessive EDA. After being stirred at RT for 12 h, the suspension was then vacuum-filtered. The filter cake was washed with much anhydrous THF at least 5 times and dried in a freeze drier, yielding diamine-modified MWNTs (D-MWNTs). The schematic of the reaction procedure is shown in Fig. 1 [13].

2.4. Fabrication of PA6/MWNT nanocomposites

PA6/MWNT nanocomposites containing 1 wt% A-MWNTs or 1 wt% D-MWNTs were fabricated via a simple melt compounding method using an HAAKE Mini-Lab twin-screw extruder (Thermo Electron Corporation) with a recycle circuit. Using a counter-rotating screw configuration, PA6/MWNT nanocomposites were processed at 230 °C for 25 min with a screw speed of 50 rpm, protected by nitrogen atmosphere. The extrudate was then continuously cooled by cold air and then pelletized. Finally, the pelletized extrudates were injection molded to form test bars using micro-injection molding machine (Thermo Electron Corporation). Injection temperature and mold temperature were 245 °C and 100 °C, respectively. For comparison, PA6 and PA6/U-MWNT nanocomposites containing 1 wt% U-MWNTs were also prepared with the same procedure.

2.5. Characterization

The surface state analysis of MWNTs after modification was conducted by XPS employing an ESCALAB250 (Thermo VG, USA) spectrometer with Al Kα (1486.6 eV) radiation. The spectrometer was run at pass energy 12 kV and 15 mA.

Apparent density test was conducted based on the Chinese National Standard GB/T 12496.1-1999. After being dried under vacuum at 80 °C for 24 h, about 300 mg of the MWNT samples was weighed accurately. Cylinder (10 ml) was used to measure the apparent volume and then the apparent density was calculated. For each apparent volume, the test must be repeated 3 times.

The microstructure transformation of MWNTs was observed using a field emission scanning electron microscope (SEM) (JEOL JSM 6301F). The morphology of the cryogenically fractured surfaces by liquid nitrogen and tensile fractured surfaces of PA6/MWNT nanocomposites was examined using an environmental scanning electron microscope (ESEM) (FEI/Phillips XL-30).

Dynamic mechanical analysis of PA6/MWNT nanocomposites was carried out on NETZSCH DMA 242C instrument (Germany). The specimen of about $40 \times 12 \times 4$ mm was mounted on the fixture. The three-point bending mode was selected. Tests were performed at 1 Hz under a controlled sinusoidal strain, and the scanning temperature range from −50 °C to 180 °C at 2 °C/min heating rate.

Tensile test was performed using Instron 8871 (UK) with a crosshead speed of 2 mm/min, according to ASTM D638 M. A 5000 N of load cell and a 25 mm of gauge length were used. For each specimen, the data reported here represent the averaged results of at least five successful tests.

Differential scanning calorimetric (DSC) measurement was conducted with a NETZSCH DSC 204 F1 instrument (Germany) protected by nitrogen atmosphere. After being dried under vacuum at 80 °C for 24 h, about 5 mg of samples was weighed accurately in an aluminum pan and melted at 250 °C for 5 min to eliminate the thermal history. Then, they were cooled to 50 °C and reheated to 250 °C. Both the heating and cooling rates were 10 °C/min.

3. Results and discussion

3.1. XPS analysis of MWNTs

Generally, XPS spectroscopy for chemical analysis could provide qualitative and quantitative information about the

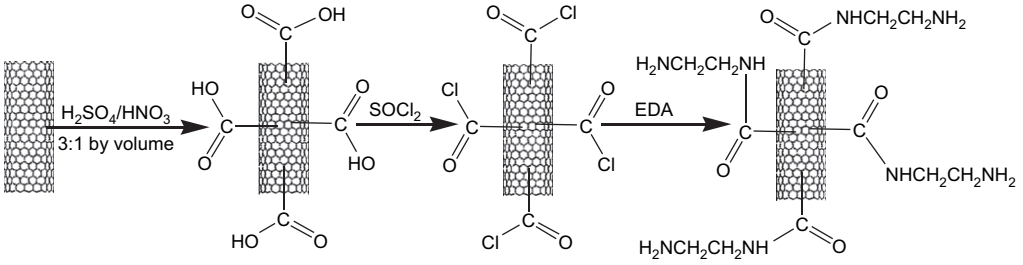

Fig. 1. Chemical routes for the preparation of A-MWNTs and D-MWNTs.

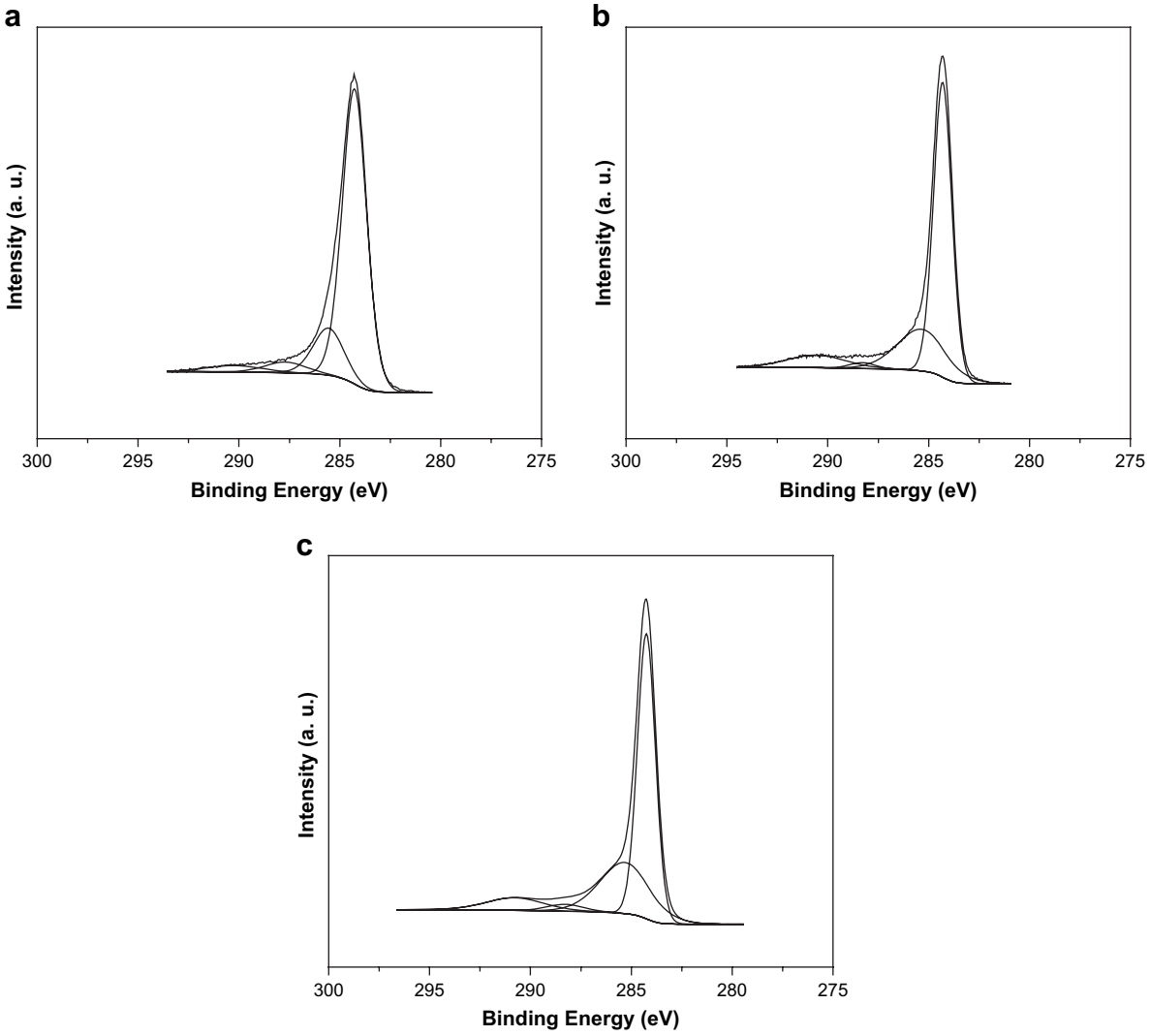

Fig. 2. C_{1s} XPS spectra of (a) U-MWNTs, (b) A-MWNTs and (c) D-MWNTs.

elemental composition of matter [41]. Therefore, XPS analysis was employed to characterize the surface state of chemically modified MWNTs in this work. Fig. 2 presents the C_{1s} XPS spectra of various MWNTs. The C_{1s} peak region of MWNTs at 284.6 eV can be deconvoluted into four fitting curves with binding energy at 285.0 eV, 286.6 eV, 288.9 eV and 291.1 eV, which are assigned to C–C, C–O, C = O and O–C=O, respectively [18]. In Fig. 2(c), C–N functional component at binding energy 285.7 eV is also fitted according to NIST database (USA). In Fig. 2, the outermost peak is the XPS spectra, the inner peaks are the deconvoluted ones according to different binding energies of different functional groups. Therefore, the percentage of functional groups is calculated based on the area under each deconvoluted peak. The relative percentage of functional components obtained from curve fitting the C_{1s} peak and elemental composition of different MWNTs are listed in Tables 1 and 2.

From Table 1, it is found that the relative percentages of C–O and O–C=O on the surface of A-MWNTs are much higher than those of U-MWNTs, especially the relative percentage of O–C=O. The atomic percentage of the oxygen element on the surface of A-MWNTs also increases obviously compared with U-MWNTs (Table 2). These results imply that acid treatment with mixed high concentration acids could effectively induce more polar oxygen-containing groups on

Table 1
Relative percentage of functional components obtained from curve fitting the C_{1s} peak of the MWNT samples

Surface functional groups and their relative percentages (%)	N–C	C–C	C–O	C=O	O–C=O
U-MWNTs	–	79.19	12.31	4.66	3.84
A-MWNTs	–	67.81	19.59	3.82	8.78
D-MWNTs	3.65	71.06	19.60	2.90	2.79

Table 2
Summary of the elemental composition of the MWNT samples

Element (at.%)	C	O	N	O/C
U-MWNTs	98.24	1.76	–	0.018
A-MWNTs	90.54	9.46	–	0.104
D-MWNTs	90.20	8.18	1.62	0.091

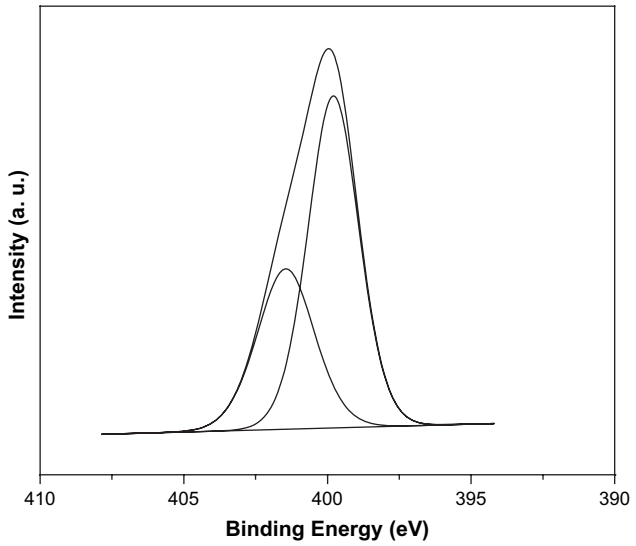

Fig. 3. N_{1s} XPS spectrum of D-MWNTs.

the surface of MWNTs, which will help MWNTs to combine with polar PA6 matrix.

The D-MWNTs (Fig. 2(c)) show a much similar spectrum to that of the A-MWNTs (Fig. 2(b)). However, a new component at 285.7 eV is attributed to the C–N emerges. The elemental composition of nitrogen element is 1.62% (Table 2), which confirms the presence of nitrogen on the surface of MWNTs after diamine modification.

Fig. 3 shows deconvoluted N_{1s} XPS spectrum of D-MWNTs. The two peaks at different binding energies indicate that there are two chemical states of N. The first one at a binding energy of 399.8 eV is attributed to the bond of O=C–NH–C, which comes from the amidation reaction between A-MWNTs and EDA; the second one at 400.7 eV represents the bond of C–C–NH_2 originating from EDA. These results are in good accordance with the schematic shown in Fig. 1, which further confirms that EDA is covalently bonded on the surface of MWNTs during diamine modification.

3.2. Apparent density of MWNTs

Fig. 4 shows the apparent volume and apparent density of MWNTs after different modifications. It is seen that the apparent density of MWNTs increases after acid treatment sharply from 53.5 mg/ml to 80.0 mg/ml. However, interestingly, the apparent density of MWNTs after further diamine modification decreases significantly down to 47.9 mg/ml, which is less than that of U-MWNTs. The results indicate that acid treatment makes MWNTs more compact stacking, while the further diamine modification may weaken the interaction among MWNTs resulting in a loose stacking of D-MWNTs. This is consistent with the results of Li et al. [42].

3.3. Microstructure transformation of MWNTs

Fig. 5 displays the typical SEM images of the U-MWNTs, A-MWNTs and D-MWNTs. It is observed that all the

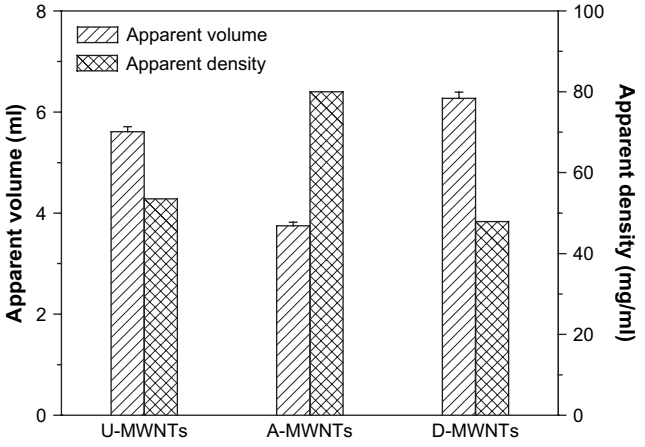

Fig. 4. Apparent volume and apparent density of MWNTs.

MWNTs are curled and entangled, but their stacking morphology is different. From Fig. 5, it is observed that the A-MWNTs have a more compact stacking morphology compared with U-MWNTs and D-MWNTs. This is perhaps due to the strong interactions between the oxygen-containing groups on the external walls and the end caps of A-MWNTs, such as the hydrogen bonds. Moreover, it is unexpected to find that after further diamine modification the stacking morphology of MWNTs changes remarkably from a compact stacking of A-MWNTs to a less compact stacking of D-MWNTs. This implies that acid treatment on the MWNTs causes a strong interaction among MWNTs and thus results in a compact stacking morphology of A-MWNTs; on the contrary, the succedent amidation process weakens the interaction among MWNTs and therefore leads to a loose stacking morphology, which is beneficial for MWNTs to disperse in PA6 matrix. These results accord with the apparent density changes of MWNTs. It is proposed that EDA molecules grafted on the surface of MWNTs resulted in the steric hindrance effect, so the interaction among the MWNTs such as the hydrogen bonds formed in acid treatment was weakened [42]. Therefore, it is expected that the D-MWNTs have better dispersion in PA6 matrix.

3.4. Dispersion of MWNTs and interfacial adhesion with PA6 matrix

Fig. 6 shows the SEM images of cryogenically fractured surfaces in liquid nitrogen for the PA6/MWNT nanocomposites. The white-dot regions represent the ends of MWNTs that were stretched out of the PA6 matrix. For the PA6/U-MWNT, the MWNT aggregates are dispersed nonuniformly in PA6 matrix and many of big aggregates can still be found (Fig. 6(a) and (b), indicated by white arrows). The dispersion of A-MWNTs is found much better than that of U-MWNTs in PA6 matrix (Fig. 6(c) and (d)). The dimension of most MWNT aggregates is less than 200 nm. Because the strong interaction among A-MWNTs such as the hydrogen bonds formed in acid treatment is unfavorable for A-MWNTs to disperse uniformly in PA6 matrix even if their polar functional groups may react with PA6 matrix. Therefore, if a further modification on

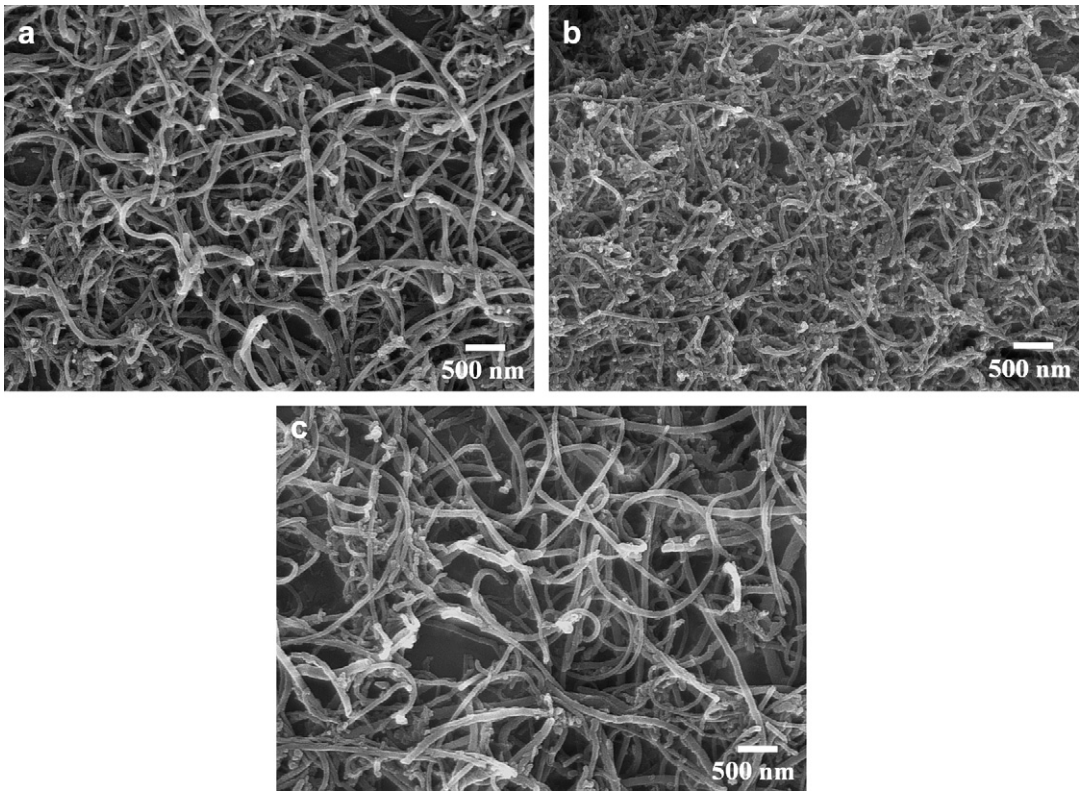

Fig. 5. SEM images of (a) U-MWNTs, (b) A-MWNTs and (c) D-MWNTs.

A-MWNTs can be done to weaken the interaction among A-MWNTs, it is expected that a better dispersion of the MWNTs in the PA6 matrix could be achieved. Fig. 6(e) and (f) demonstrates a better dispersion of the MWNTs after a further diamine modification on A-MWNTs. This proves the above assumption. After diamine modification, the strong interaction among A-MWNTs such as the hydrogen bonds is undermined partly leading to a less compact stacking, which is helpful for the dispersion of D-MWNTs in the PA6 matrix. From Fig. 6, it can be seen that modified MWNTs have a better dispersion as compared to U-MWNTs in the PA6 matrix, especially D-MWNTs. In a word, D-MWNTs have a better dispersion in PA6 matrix as compared to U-MWNTs and A-MWNTs.

Fig. 7 presents the SEM images of tensile fractured surfaces of PA6/MWNT nanocomposites. In Fig. 7(a) and (b), the aggregation and pull-apart shape of U-MWNTs resulting from the incompatibility of the U-MWNTs and PA6 matrix can be observed, which agrees with the observations on the cryogenically fractured surface. Moreover, it is found that the pullout of U-MWNTs is the dominant failure mechanism, which indicates the weaker interfacial adhesion between U-MWNTs and PA6 matrix. By contrast to U-MWNTs, it is seen from Fig. 7(c) to (f) that both A-MWNTs and D-MWNTs are effectively dispersed in the PA6 matrix, because the polar oxygen-containing groups and diamine groups on the surface of modified MWNTs probably have reacted with PA6 in melt-mixing process resulting in better dispersion state and stronger interfacial adhesion. From Fig. 7(c) to (f), MWNTs' pullout is minimal and the plastic deformation of PA6 matrix becomes the dominant failure mechanism. This implies that there are improved interfacial adhesion between modified MWNTs and PA6 matrix.

3.5. DMA analysis

Fig. 8(a) shows the dynamic storage modulus (E') versus temperature of various PA6/MWNT nanocomposites. From Fig. 8(a), it can be found that the incorporation of MWNTs increases E' of PA6 significantly almost at all temperatures, especially below the glass transition temperature (T_g), which is due to the stiffening effect of the MWNTs. The E' increases in the order of PA6/U-MWNT, PA6/A-MWNT and PA6/D-MWNT nanocomposites, which results from the fact that the D-MWNTs have better dispersion and stronger interfacial adhesion with PA6 matrix than the other MWNTs. As seen in Table 3, the E' of PA6 at 0 °C is improved obviously due to the extremely high modulus of MWNTs.

Fig. 8(b) presents the temperature dependence of the loss tangent ($\tan\delta$) of PA6 and PA6/MWNT nanocomposites. Apart from PA6/U-MWNT nanocomposite, the position of the loss tangent peak for the nanocomposites obviously shifts toward high temperature as compared to PA6, which indicates that the T_g of PA6 rises (Table 3). On the contrary, the T_g of PA6/U-MWNT nanocomposite decreases compared with PA6. It is well known that in polymer matrix composites, the T_g of the polymer matrix depends on the free volume of the polymer, which is related to the affinity between the filler and the polymer matrix [22,43]. As seen from SEM images,

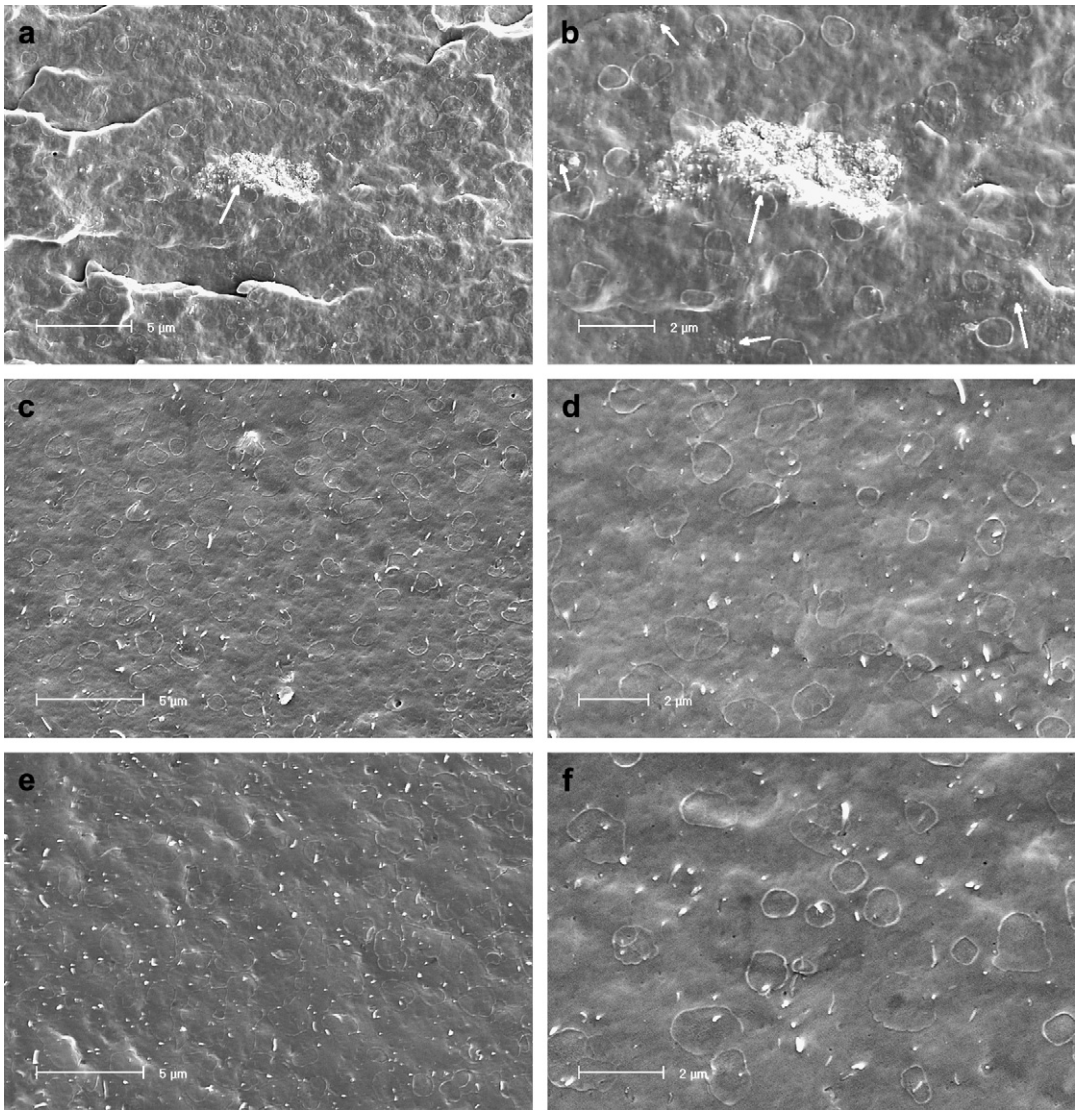

Fig. 6. SEM images of cryogenically fractured surface for (a and b) PA6/U-MWNT, (c and d) PA6/A-MWNT and (e and f) PA6/D-MWNT.

the U-MWNTs have a worse affinity with the PA6 matrix, which leads to a large free volume beyond that of PA6, and hereby results in a lower T_g of the PA6/U-MWNT nanocomposite than that of PA6. Because the modified MWNTs have better dispersion and stronger affinity with the PA6 matrix, the free volume of the corresponding nanocomposites decreases and then the T_g rises. Due to better dispersion and stronger affinity with PA6 matrix of D-MWNTs, the T_g of the PA6/D-MWNT nanocomposite is high.

3.6. Tensile properties

Fig. 9 is the typical tensile stress–strain curves for PA6 and PA6/MWNT nanocomposites. Due to the elongation limitation of extensometer, only part of the curve is automatically recorded by computer. From Fig. 9, one can see that a pronounced yield and post-yield drop are featured for all curves.

The tensile properties of PA6 and PA6/MWNT nanocomposites are summarized in Table 4. Obviously, the addition of U-MWNTs almost has no reinforcing effect on PA6 and just enhances the Young's modulus of PA6 slightly. In sharp contrast, it can be seen that the yield strength and Young's modulus of PA6 were greatly improved by the incorporation of A-MWNTs and D-MWNTs, especially D-MWNTs. However, the elongation at break of PA6 decreases due to the addition of the MWNTs, especially U-MWNTs, which indicates that the nanocomposites become somewhat brittle compared with the PA6 matrix.

It is well known that the mechanical properties of PA6/MWNT nanocomposites depend on the dispersion of MWNTs in PA6 matrix and the interfacial adhesion between the MWNTs and PA6 matrix. From the above discussion, it is found that the U-MWNTs have an aggregation of high extent and a weak interfacial adhesion with PA6 matrix. The aggregation plays the role of microdefect in the nanocomposite and therefore results in low tensile strength and low elongation at break of PA6/U-MWNT nanocomposites. Contrarily, A-MWNTs and D-MWNTs have more uniform dispersion and

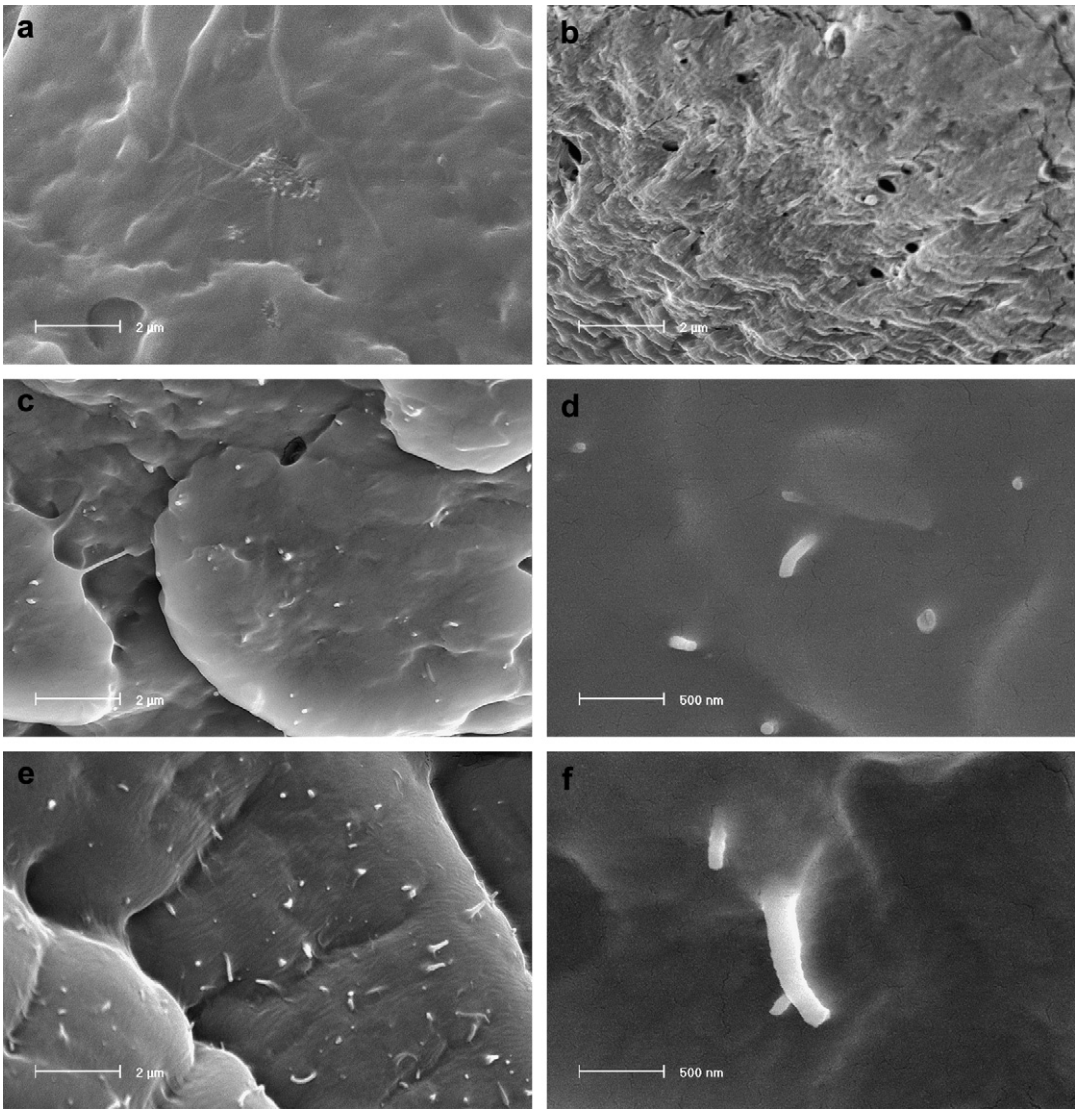

Fig. 7. SEM images of tensile fractured surfaces of (a and b) PA6/U-MWNT, (c and d) PA6/A-MWNT and (e and f) PA6/D-MWNT.

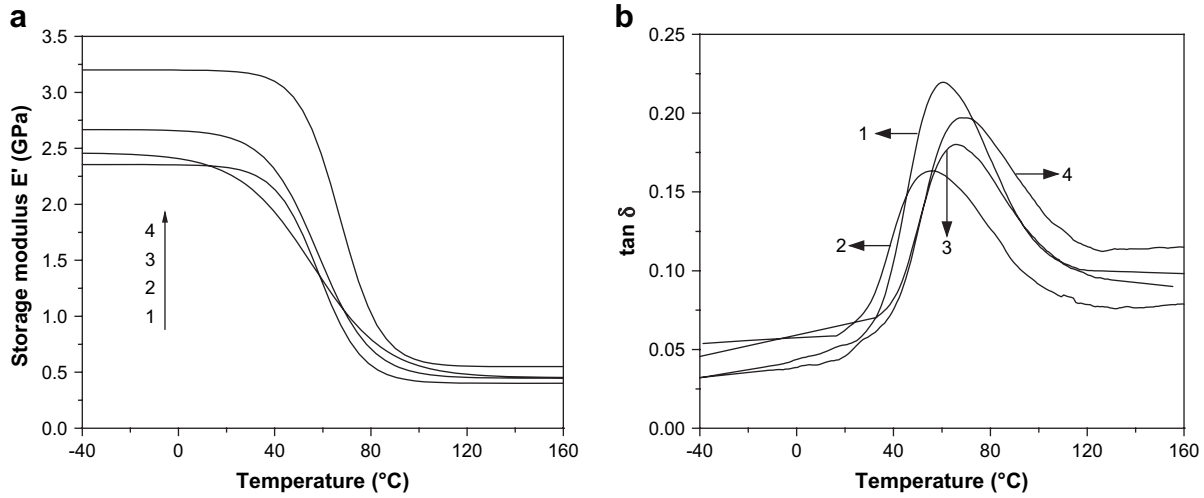

Fig. 8. (a) Storage modulus E' and (b) the loss tangent tan δ versus temperature curves for (1) PA6, (2) PA6/U-MWNT, (3) PA6/A-MWNT and (4) PA6/D-MWNT.

Table 3
Dynamic mechanical properties of PA6 and PA6/MWNT nanocomposites

Sample	E' at 0 °C (GPa)	T_g (°C)
PA6	2.3	60.5
PA6/U-MWNT	2.4	55.3
PA6/A-MWNT	2.7	66.3
PA6/D-MWNT	3.2	69.1

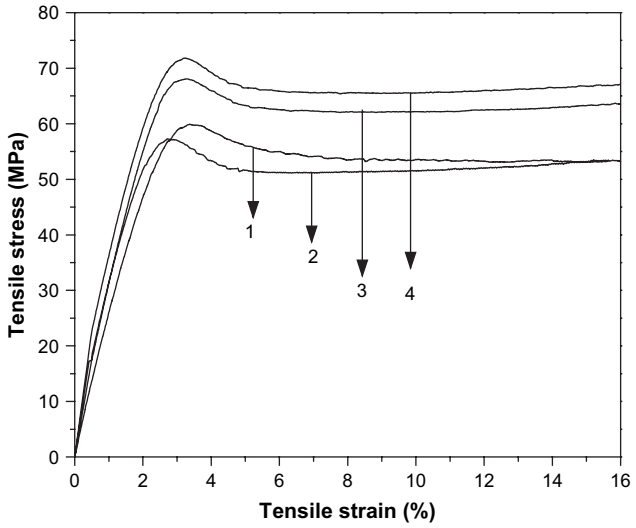

Fig. 9. Typical tensile stress–strain curves of (1) PA6, (2) PA6/U-MWNT, (3) PA6/A-MWNT and (4) PA6/D-MWNT.

Table 4
Tensile properties of PA6 and PA6/MWNT nanocomposites

Sample	Yield strength (MPa)	Young's modulus (GPa)	Elongation at break (%)
PA6	60.4 ± 0.8	3.3 ± 0.1	151 ± 18
PA6/U-MWNT	57.2 ± 1.0	3.5 ± 0.1	78 ± 13
PA6/A-MWNT	67.7 ± 0.9	4.2 ± 0.2	109 ± 15
PA6/D-MWNT	71.5 ± 1.1	4.7 ± 0.3	121 ± 21

stronger interfacial adhesion with PA6 matrix, so the corresponding nanocomposites have higher tensile properties. Due to high dispersion in PA6 matrix the D-MWNTs have higher reactivity opportunity with PA6 matrix, resulting in stronger interfacial adhesion; therefore the PA6/D-MWNT nanocomposites have the highest tensile strength and elongation at break among the three kinds of nanocomposites. However, it is noticed that the dispersion of D-MWNTs in the PA6 matrix is still not in a nanometer scale, some aggregations still exist; in addition, the inclusion of the D-MWNTs also restricts the motion of PA6 chains physically or chemically, therefore the elongation at break of PA6/D-MWNT nanocomposites is less than that of PA6.

3.7. Crystallization behavior

It is recognized that crystallization behavior of semi-crystalline polymers has a significant influence on the mechanical properties of their composites. Therefore, it is very important to investigate the effect of MWNTs with a high aspect ratio on the crystallization behavior of PA6. The DSC thermograms are shown in Fig. 10 and the obtained parameters are given in Table 5. From Fig. 10(a), it can be found that the crystallization peaks of nanocomposites shift to a higher temperature with the incorporation of MWNTs compared with PA6, which indicates that the crystallization temperature (T_c) rises. As shown in Table 5, the incorporation of MWNTs results in a rise of T_c for all nanocomposite systems, which suggests that all the MWNTs act as effective heterogeneous nucleating agents for PA6. Furthermore, the PA6 nanocomposites containing A-MWNTs and D-MWNTs have a bigger rise of T_c as compared to the PA6/U-MWNT nanocomposites, which is attributed to the fact that the modified MWNTs, especially D-MWNTs, have a better dispersion in PA6 matrix compared with U-MWNTs. Moreover, the crystallization peak of PA6 is sharper than those of all the nanocomposites, indicating that the addition of MWNTs influences the perfect degree of crystal of PA6. From Fig. 10(b), one can see that MWNTs almost have no influence on the melting point (T_m) of PA6.

In this work, the degree of crystallinity (X_c) for PA6 and PA6/MWNT nanocomposites was calculated from the

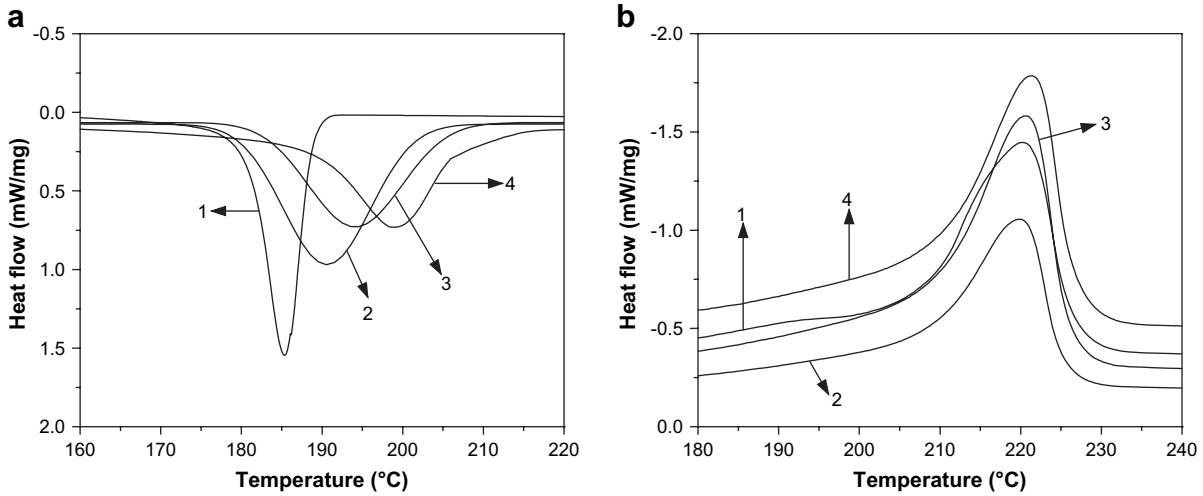

Fig. 10. DSC thermograms of (a) crystallization and (b) secondary melting for (1) PA6, (2) PA6/U-MWNT, (3) PA6/A-MWNT and (4) PA6/D-MWNT.

Table 5
Crystallization parameters of PA6 and PA6/MWNT nanocomposites

Sample	T_m (°C)	T_c (°C)	ΔH_c (J/g)	X_c (%)
PA6	220.5	185.4	60.30	31.74
PA6/U-MWNT	220.1	190.5	69.62	37.01
PA6/A-MWNT	220.9	194.7	67.42	35.84
PA6/D-MWNT	221.5	198.9	64.33	34.20

enthalpy evolved during crystallization based on the cooling scans using the following formula:

$$X_c\,(\%) = \frac{\Delta H_c}{(1-\phi)\Delta H_m^0} \times 100 \quad (1)$$

where ΔH_c is the apparent enthalpy of crystallization of sample, ΔH_m^0 is the extrapolated value of the enthalpy corresponding to the melting of 100% crystalline PA6, which is taken as 190 J/g, and ϕ is the weight fraction of MWNTs in the composites [44–46]. From Table 5 it is evident that additions of all the MWNTs do increase X_c of PA6, but the X_c increases in the order of PA6/D-MWNT, PA6/A-MWNT and PA6/U-MWNT nanocomposites.

Generally, the inorganic fillers have two inconsistent influences on the crystallization of the semi-crystalline polymers. On the one hand, they act as heterogeneous nucleating agents to facilitate the crystallization of polymers; on the other hand, they hinder the motion of polymer chain segments to retard the crystallization of polymers [47]. As mentioned earlier, after chemical modifications there are stronger interactions between MWNTs and PA6, so the hindering effect of MWNTs is dominant, which results in a lower X_c of modified MWNT/PA6 nanocomposites compared with PA6/U-MWNT nanocomposites, especially PA6/D-MWNT nanocomposites.

As known, semi-crystalline polymers always have two-phase structure, i.e. crystalline and amorphous phases. Normally, the strength of the former is higher than that of the latter. Consequently, for a given polymer, it is evident that higher degree of crystallinity often implies stronger mechanical properties. Moreover, the mechanical properties of semi-crystalline polymer matrix composites also depend on the dispersion of fillers and the interfacial adhesion between the fillers and the polymer matrix. On the one hand, a stronger interfacial adhesion will hinder polymer crystallization during processing, which results in a lower degree of crystallinity of polymer matrix and decreases the mechanical properties of polymer matrix. On the other hand, a stronger interfacial adhesion also ensures the efficient load transfer from polymer matrix to the fillers, which leads to high mechanical properties of composites. Therefore, the mechanical properties of the semi-crystalline polymer matrix composites would be determined by the two competitive aspects. As to PA6/U-MWNT and PA6/D-MWNT nanocomposites, although the former have higher degree of crystallization, the latter have stronger mechanical properties due to stronger interfacial adhesion. In a word, in this work the effect of interfacial adhesion on the mechanical properties of PA6/MWNT nanocomposites is more powerful than that of the degree of crystallinity.

4. Conclusions

In this work, the effects of acid- and diamine-modified MWNTs on the mechanical properties and crystallization behavior of PA6 were investigated. Some conclusions can be drawn as follows.

1. Acid treatment of MWNTs using mixed concentrated sulfuric acid and concentrated nitric acid as well as the further modification of acid-modified MWNTs with ethylenediamine (EDA) was effective to graft polar oxygen-containing groups and diamine groups on the surface of MWNTs. The strong interaction among MWNTs such as the hydrogen bonds from the polar oxygen-containing groups led to a compact stacking morphology of the acid-modified MWNTs. After further modification of acid-modified MWNTs with EDA, the EDA molecules grafted on the surface of MWNTs resulted in the steric hindrance effect and weakened the interaction among MWNTs, which produced the less compact stacking morphology of the diamine-modified MWNTs. Therefore, diamine-modified MWNTs had better dispersion and stronger interfacial adhesion with PA6 matrix compared with acid-modified MWNTs.
2. The acid-modified MWNTs and diamine-modified MWNTs were potent reinforcements for PA6. The storage modulus, glass transition temperature, yield strength and Young's modulus of PA6 were improved significantly by the incorporation of modified MWNTs. Compared with acid-modified MWNTs, diamine-modified MWNTs had higher reinforcing efficiency for PA6, which could be attributed to the better dispersion of diamine-modified MWNTs and stronger interfacial adhesion between diamine-modified MWNTs and PA6 matrix.
3. The acid-modified MWNTs and diamine-modified MWNTs acted as effective heterogeneous nucleating agents for PA6 and thus resulted in an increase in the crystallization temperature and the degree of crystallinity of PA6. Compared with the acid-modified MWNT/PA6 nanocomposites, the diamine-modified MWNT/PA6 nanocomposites had higher crystallization temperature due to better dispersion of the diamine-modified MWNTs and lower degree of crystallinity due to the hindering effect from the stronger interaction between diamine-modified MWNTs and PA6.

Acknowledgements

G.X.S. would like to acknowledge the financial supports of the Hundreds' Talents Program of Chinese Academy of Sciences and of the Scientific Research Foundation for the Returned Overseas Chinese Scholars, Chinese Ministry of Education.

References

[1] Iijima S. Nature 1991;354(6348):56–8.
[2] Ajayan PM, Stephan O, Colliex C, Tranth D. Science 1994;265(5176):1212–4.

[3] Calvert P. Nature 1999;399(6733):210–1.
[4] Thostenson ET, Ren Z, Chou T-W. Compos Sci Technol 2001;61(13): 1899–912.
[5] Lau K-T, Hui D. Compos Part B Eng 2002;33(4):263–77.
[6] Andrews R, Weisenberger MC. Curr Opin Solid State Mater 2004;8(1): 31–7.
[7] Szleifer I, Yerushalmi-Rozen R. Polymer 2005;46(19):7803–18.
[8] Lu JP. J Phys Chem Solids 1997;58(11):1649–52.
[9] Li F, Cheng HM, Bai S, Su G, Dresselhaus MS. Appl Phys Lett 2000; 77(20):3161–3.
[10] Kwon J-Y, Kim H-D. J Appl Polym Sci 2005;96(2):595–604.
[11] Shao W, Wang Q, Wang F, Chen Y. Carbon 2006;44(13):2708–14.
[12] Zhao C, Hu G, Justice R, Schaefer DW, Zhang S, Yang M, et al. Polymer 2005;46(14):5125–32.
[13] Xiong J, Zheng Z, Qin X, Li M, Li H, Wang X. Carbon 2006;44(13): 2701–7.
[14] Zeng H, Gao C, Wang Y, Watts PCP, Kong H, Cui X, et al. Polymer 2006;47(1):113–22.
[15] Zhang WD, Shen L, Phang IY, Liu T. Macromolecules 2004;37(2):256–9.
[16] Wu H-L, Wang C-H, Ma C-CM, Chiu Y-C, Chiang M-T, Chiang C-L. Compos Sci Technol 2007;67(9):1854–60.
[17] Liu T, Tong Y, Zhang W-D. Compos Sci Technol 2007;67(37–4):406–12.
[18] Chen L, Pang X-J, Qu M-Z, Zhang Q-T, Wang B, Zhang B-L, et al. Compos Part A Appl Sci Manuf 2006;37(9):1485–9.
[19] Gojny FH, Nastalczyk J, Roslaniec Z, Schulte K. Chem Phys Lett 2003;370(5–6):820–4.
[20] Shen J, Huang W, Wu L, Hu Y, Ye M. Compos Part A Appl Sci Manuf 2007;38(5):1331–6.
[21] Wang M, Pramoda KP, Goh SH. Polymer 2005;46(25):11510–6.
[22] Yuen S-M, Ma C-CM, Lin Y-Y, Kuan H-C. Compos Sci Technol 2007; 67(11–12):2564–73.
[23] Jin J, Song M, Pan F. Thermochim Acta 2007;456(1):25–31.
[24] Paiva MC, Zhou B, Fernando KAS, Lin Y, Kennedy JM, Sun Y-P. Carbon 2004;42(14):2849–54.
[25] Ruan SL, Gao P, Yang XG, Yu TX. Polymer 2003;44(19):5643–54.
[26] Lin Y, Zhou B, Fernando KAS, Liu P, Allard LF, Sun Y-P. Macromolecules 2003;36(19):7199–204.
[27] Jin Z, Pramoda KP, Xu G, Goh SH. Chem Phys Lett 2001;337(1–3): 43–7.
[28] Liu I-C, Huang H-M, Chang C-Y, Tsai H-C, Hsu C-H, Tsiang RC-C. Macromolecules 2004;37(2):283–7.
[29] Shaffer MSP, Windle AH. Adv Mater 1999;11(11):937–41.
[30] Zhou Z, Wang S, Lu L, Zhang Y, Zhang Y. Compos Sci Technol 2007; 67(9):1861–9.
[31] Zou Y, Feng Y, Wang L, Liu X. Carbon 2004;42(2):271–7.
[32] Kang M, Myung SJ, Jin H-J. Polymer 2006;47(11):3961–6.
[33] Pötschke P, Brünig H, Janke A, Fischer D, Jehnichen D. Polymer 2005; 46(23):10355–63.
[34] McNally T, Pötschke P, Halley P, Murphy M, Martin D, Bell SEJ, et al. Polymer 2005;46(19):8222–32.
[35] Kashiwagi T, Fagan J, Douglas JF, Yamamoto K, Heckert AN, Leigh SD, et al. Polymer 2007;48(16):4855–66.
[36] Li X, Huang YD, Liu L, Cao HL. J Appl Polym Sci 2006;102:2500–8.
[37] Zou H, Wang K, Zhang Q, Fu Q. Polymer 2006;47(22):7821–6.
[38] Bose S, Bhattacharyya AR, Kodgire PV, Misra A. Polymer 2007;48(1): 356–62.
[39] Wei H-F, Hsiue G-H, Liu C-Y. Compos Sci Technol 2007;67:1018–26.
[40] Kim JY, Park HS, Kim SH. Polymer 2006;47(4):1379–89.
[41] Watts JF, Wolstenholme J. An introduction to surface analysis by XPS and AES. Chichester, England: John Wiley & Sons Ltd; 2003.
[42] Li J, Fang ZP, Wang JG, Gu AJ, Tong LF, Liu F. Acta Phys Chim Sin 2005;21(11):1244–8.
[43] Menard KP. Dynamic mechanical analysis. Boca Raton, Florida: CRC Press; 1999.
[44] Campoy I, Gómez MA, Marco C. Polymer 1998;39(25):6279–88.
[45] Wu Q, Liu X, Berglund LA. Macromol Rapid Commun 2001;22(17): 1438–40.
[46] Xie S, Zhang S, Liu H, Chen G, Feng M, Qin H, et al. Polymer 2005; 46(14):5417–27.
[47] Kuo MC, Huang JC, Chen M. Mater Chem Phys 2006;99(2–3):258–68.